

Electronic Supplementary Information (ESI)

**Novel efficient blue and bluish-green light-emitting polymers with
delayed fluorescence**

Yingyuan Hu,[‡] Wanqing Cai,[‡] Lei Ying*, Dongjun Chen, Xiye Yang, Xiao-Fang Jiang, Shijian Su, Fei Huang*, and Yong Cao

Table of Contents

1. Experimental Section	2-4
General Details.....	2
Synthesis and Characterization	2-4
2. Determination of Φ_{RISC}, Φ_{ISC}, ΔE_{ST}, Rate Constants	5
References.....	5
3. Physical Properties	6-14
4. Device Fabrication and Performance	15-16
5. NMR and MS Spectra.....	17-23

1. Experimental Section

General Details

^1H and ^{13}C NMR spectra were measured on a Bruker NMR spectrometer operating at 500 and 126 MHz, respectively, using tetramethylsilane (TMS) as the internal standard. Chemical shifts were expressed in parts per million (ppm), and splitting patterns are designated as s (singlet), d (doublet) and m (multiplet). LC-MS data was obtained on a Bruker Esquire HCT PLUS with atmospheric pressure chemical ionization resource (APCI). MALDI-TOF-MS was measured using a Waters SYNAPT G2-Si. Molecular weights of the polymers were determined by a Waters GPC 2410 in THF using a calibration curve with polystyrene standards. Thermogravimetric analyses (TGA) were conducted on a NETZSCH TG 209 under a heating rate of 10 °C/min and a N_2 flow rate of 20 mL/min. Cyclic voltammetry data were measured on a CHI600D electrochemical workstation by using Bu_4NPF_6 (0.1 M) in acetonitrile as electrolyte and platinum and saturated calomel electrode as the working and reference electrode, respectively. Atomic force microscopy (AFM) measurements were carried out using a Digital Instrumental DI Multimode Nanoscope IIIa in tapping mode.

Synthesis and Characterization

All reagents, unless otherwise specified, were obtained from Alfa Aesar or Sigma-Aldrich and used without further purification. Some of the solvents used were further purified before use (toluene was washed with H_2SO_4 and then treated with CaCl_2).

4-Octyloxyacetanilide (1): 1-bromooctane (144.84 g, 750 mmol) and K_2CO_3 (138.21 g, 1000 mmol) were added to 4-acetamidophenol (75.6 g, 500 mmol) dissolved in 750 mL acetone. The solution was stirred vigorously for 24 h under reflux. The resulting mixture was washed with excess of water, and the white precipitate was filtered off. Then, the crude product was dried, and purified by recrystallization from THF/petroleum ether to give **1** as a white solid (yield = 109.6 g, 83.2%). ^1H NMR (500 MHz, CDCl_3): δ 7.39–7.28 (m, 3H), 6.83 (d, J = 8.9 Hz, 2H), 3.93 (t, J = 13.2 Hz, 6.5 Hz, 2H), 2.14 (s, 3H), 1.82–1.71 (m, 2H), 1.46–1.24 (m, 10H), 0.89 (t, J = 7.0 Hz, 3H). ^{13}C NMR (126 MHz, CDCl_3): δ 170.69, 156.59, 132.38, 120.99, 115.80, 69.66, 31.73, 29.15, 29.04, 28.80, 26.58, 23.82, 23.16, 14.00. LC-MS (m/z): $[\text{M}]^+$ calculated for $\text{C}_{16}\text{H}_{25}\text{NO}_2$, 263.38; found, 263.5.

4-Octyloxyaniline (2): **1** was dissolved in 600 mL ethanol, and 219 mL concentrated hydrochloric acid was added dropwise. The reaction solution was stirred for 24 h under reflux. The resulting claret-red mixture was cooled to ambient temperature and then poured over 500g ice, white precipitate was generated. After the solution was neutralized to pH 7-8 with NaOH solution, the precipitate was filtered off, and washed with water, after dried in vacuum oven, **2** was obtained as a white solid (yield = 60.6 g, 65.8%). ^1H NMR (500 MHz, $\text{DMSO}-d_6$): δ 6.64–6.59 (m, 2H), 6.51–6.46 (m, 2H), 4.57 (s, 2H), 3.79 (t, J = 6.5 Hz, 2H), 1.67–1.58 (m, 2H), 1.43–1.17 (m, 10H), 0.86 (t, J = 7.0 Hz, 3H). ^{13}C NMR (126 MHz, $\text{DMSO}-d_6$): δ 150.47, 142.74, 115.78, 115.39, 68.34, 31.72, 29.40, 29.27, 29.16, 26.07, 22.56, 14.43. LC-MS (m/z): $[\text{M}]^+$ calculated for $\text{C}_{14}\text{H}_{23}\text{NO}$, 221.34; found, 221.6.

Di(4-bromophenyl)sulfide (3): Diphenylsulfide (16.5 mL, 100 mmol) was dissolved in a mixed solution of CH_2Cl_2 and H_2O (1:1, 300 mL). Then 30% hydrogen peroxide (5.6 mL, 180 mmol) and bromine (20.5 mL, 400 mmol) were added, and the reaction solution was continuously stirred for 4 h. The resulting mixture was extracted with CH_2Cl_2 with surplus bromine removed by saturated Na_2SO_3 solution. After removing the CH_2Cl_2 solvent, the residue was further purified by silica gel column chromatography (petroleum ether) to give **3** as a white solid (yield = 31.7 g, 92.2%). ^1H NMR (500 MHz, CDCl_3): δ 7.47–7.40 (d, 4H), 7.22–7.16 (d, 4H). ^{13}C NMR (126 MHz, CDCl_3): δ 134.49, 132.60, 132.46, 121.51. LC-MS (m/z): $[\text{M}]^+$ calculated for $\text{C}_{12}\text{H}_8\text{Br}_2\text{S}$, 344.06; found, 344.4.

4,4'-Dibromo diphenyl sulfone (4): **3** (11.7 g, 34.1 mmol) was dissolved in 150 mL acetic acid under argon atmosphere. Then 150 mL 30% aqueous hydrogen peroxide were added, and the reaction solution was continuously stirred for about 6 h at 80 °C. The completion of the reaction was verified by spot TLC. The

resulting mixture was extracted with CH₂Cl₂ with surplus acetic acid removed by Na₂CO₃. After removing the CH₂Cl₂ solvent, the residue was further purified by repeated recrystallization from ethanol to afford **4** as a white solid (yield = 11.3 g, 88.5%). ¹H NMR (500 MHz, CDCl₃): δ 7.82–7.75 (d, 4H), 7.68–7.62 (d, 4H). ¹³C NMR (126 MHz, CDCl₃): δ 140.23, 132.78, 129.19, 128.83. LC-MS (m/z): [M+H]⁺ calculated for C₁₂H₈Br₂O₂S, 376.06; found, 377.3.

4,4'-Sulfonylbis(N-(4-(octyloxy)phenyl)aniline) (5): A catalyst consisting of tris(dibenzylideneacetone)-dipalladium(0) (Pd₂dba₃) (0.385 g, 0.42 mmol) and diphenylphosphinoferrocene (DPPF) (0.699 g, 1.26 mmol) dissolved in 50 mL toluene and preformed by stirring for 10 min at room temperature was added to **4** (3.76 g, 10 mmol), **2** (4.65 g, 21 mmol), and sodium *tert*-butoxide (6.05 g, 63 mmol) dissolved in 150 mL toluene. This mixture was stirred for 12 h at 95 °C and then cooled to room temperature, diluted with water, and extracted with CH₂Cl₂. The organic phase was dried with MgSO₄, and the solvent was evaporated. The residue was further purified by repeated silica gel column chromatography (petroleum ether/ethyl acetate, 6:1) to give **5** as a pale yellow solid (yield = 5 g, 76%). ¹H NMR (500 MHz, DMSO-*d*₆): δ 8.54 (s, 2H), 7.60–7.56 (d, 4H), 7.10–7.05 (d, 4H), 6.92–6.86 (m, 8H), 3.92 (t, J = 6.5 Hz, 4H), 1.73–1.65 (m, 4H), 1.44–1.21 (m, 20H), 0.88–0.84 (t, 6H). ¹³C NMR (126 MHz, DMSO-*d*₆): δ 155.34, 150.11, 133.84, 130.32, 129.20, 123.61, 115.67, 113.42, 68.09, 31.72, 29.23, 29.22, 29.15, 26.02, 22.56, 14.43. MALDI-TOF-MS (m/z): [M]⁺ calculated for C₄₀H₅₂N₂O₄S, 656.93; found, 656.3502; [M+Na]⁺ calculated for C₄₀H₅₂N₂O₄S+Na, 679.93; found, 679.3373.

4-(4,6-Diphenyl-1,3,5-triazin-2-yl)-N,N-diphenylaniline (6):

Tetrakis(triphenylphosphine)palladium(0) (Pd(PPh₃)₄) (0.18 g, 0.15 mmol), 2M Na₂CO₃ (10 mL), ethanol (10 mL) and toluene (100 mL) were added to a 250 mL three-necked flask under nitrogen. 2-chloro-4,6-diphenyl-1,3,5-triazine (1.34 g, 5 mmol) and N,N-diphenyl-4-(4,4,5,5-tetramethyl-1,3,2-dioxaborolan-2-yl)aniline (2.41 g, 6.5 mmol) was added to the solution and heated to 90 °C for 6 h. After cooling to room temperature, the reaction mixture was diluted with CH₂Cl₂ and the organic phase was washed with water. After drying over MgSO₄, the solvent was removed. The resulting crude product was further purified by silica gel column chromatograph (petroleum ether/CH₂Cl₂, 3:1) and recrystallized from THF/petroleum ether to obtain **6** as a light yellow solid (yield = 1.84 g, 77.3%). ¹H NMR (500 MHz, DMSO-*d*₆): δ 8.73–8.68 (d, 4H), 8.61–8.56 (d, 2H), 7.72–7.68 (m, 2H), 7.67–7.62 (m, 4H), 7.44–7.40 (m, 4H), 7.21 (m, J = 7.8 Hz, 1.4 Hz, 6H), 7.08–7.04 (d, 2H). ¹³C NMR (126 MHz, DMSO-*d*₆): δ 171.18, 169.70, 152.17, 146.56, 136.06, 133.38, 130.77, 130.39, 129.42, 129.05, 126.22, 125.30, 120.25. LC-MS (m/z): [M]⁺ calculated for C₃₃H₂₄N₄, 476.58; found, 476.7.

4-Bromo-N-(4-bromophenyl)-N-(4-(4,6-diphenyl-1,3,5-triazin-2-yl)phenyl)aniline (7): To a stirred solution of **6** (1.84 g, 3.86 mmol) in dry THF (32 mL) was added *N*-bromosuccinimide (1.65 g, 9.26 mmol) slowly at 0 °C. The mixture was stirred for 24 h at room temperature. The reaction mixture was then poured into water, and extracted with CH₂Cl₂. The organic phase was washed with water, and then dried over MgSO₄. After filtration and evaporation, the crude product was recrystallized from THF/methanol to afford **7** as a pale yellow solid (yield = 1.79 g, 73%). ¹H NMR (500 MHz, CDCl₃): δ 8.77–8.73 (d, 4H), 8.63 (d, J = 8.7 Hz, 2H), 7.63–7.53 (m, 6H), 7.45–7.40 (m, 4H), 7.16 (d, J = 8.7 Hz, 2H), 7.07–7.03 (m, 4H). ¹³C NMR (126 MHz, CDCl₃): δ 171.47, 170.94, 150.83, 145.72, 136.34, 132.71, 132.45, 130.42, 130.14, 128.91, 128.63, 126.76, 121.92, 117.05. LC-MS (m/z): [M+H]⁺ calculated for C₃₃H₂₂Br₂N₄, 634.38; found, 635.5.

N¹-(4-(4,6-diphenyl-1,3,5-triazin-2-yl)phenyl)-N⁴-phenyl-N¹-(4-(phenylamino)phenyl)benzene-1,4-

diamine (8): A catalyst consisting of tris(dibenzylideneacetone)-dipalladium(0) (Pd₂dba₃) (0.1154 g, 0.126 mmol) and diphenylphosphinoferrocene (DPPF) (0.2096 g, 0.378 mmol) dissolved in 10 mL toluene and preformed by stirring for 10 min at room temperature was added to **7** (1.903 g, 3 mmol), aniline (1 mL, 11 mmol), and sodium *tert*-butoxide (1.816 g, 18.9 mmol) dissolved in 50 mL toluene. This mixture was stirred for 12 h at 95 °C and then cooled to room temperature, diluted with water, and extracted with CH₂Cl₂. The organic phase was dried with MgSO₄, and the solvent was evaporated. The residue was further purified by repeated recrystallized from THF/petroleum ether to give **8** as a pale yellow solid (yield = 1.48 g, 75%). ¹H NMR (500 MHz, DMSO-*d*₆): δ 8.70 (dd, J = 8.3 Hz, 1.3 Hz, 4H), 8.53 (d, J = 9.0 Hz, 2H), 8.26 (s, 2H), 7.69 (m, 2H), 7.66–7.62 (m, 4H), 7.25 (m, J = 8.4 Hz, 7.4 Hz, 4H), 7.18–7.08 (m, 12H), 6.93 (d, J = 9.0 Hz, 2H),

6.84 (m, 2H). ¹³C NMR (126 MHz, DMSO-*d*₆): δ 171.03, 170.97, 153.16, 143.78, 141.48, 138.13, 136.19, 133.22, 130.70, 129.68, 129.34, 128.97, 128.10, 125.34, 120.26, 118.29, 117.30, 116.96. MALDI-TOF-MS (m/z): [M]⁺ calculated for C₄₅H₃₄N₆, 658.81; found, 658.2638.

General procedures of C-N-Coupling copolymerization taking P1 as an example.

P1: Tris(dibenzylideneacetone)dipalladium(0) (Pd₂dba₃) (11.4 mg, 0.0125 mmol) and tris(*tert*-butyl)phosphine (15.2 mg, 0.075 mmol) were dissolved in 2 mL toluene under argon and stirred for 10 min at room temperature. This activated catalyst was then added to a mixture of **4** (0.1881 g, 0.5 mmol), **5** (0.312 g, 0.475 mmol), **8** (0.0165 g, 0.025 mmol) and sodium *tert*-butoxide (0.1441 g, 1.5 mmol) in 18 mL toluene. The reaction mixture was stirred for 18 h at 100 °C, and then 10 mL toluene was added. For end-capping purposes, first diphenylamine (90 mg, 0.53 mmol) and 5 h later bromobenzene (0.1 mL, 0.96 mmol) were added. After another 5 h, the mixture was cooled to 75 °C and 8 mL aqueous diethyldithiocarbamate solution (5% w/w) were added. The reaction mixture was stirred vigorously for 24 h and then poured into water and extracted with CH₂Cl₂. The combined organic layers were washed with water and dried over MgSO₄. After filtration and evaporation, the polymer was then precipitated by dropping the organic phase into a 10-fold excess of methanol and dried under vacuum to give **P1** as a yellow solid (yield = 364 mg, 83.6%). This compound was then further purified by silica gel column chromatography. ¹H NMR (500 MHz, CDCl₃): δ 8.74 (d, J = 6.9 Hz, 0.26H), 8.65 (d, J = 8.8 Hz, 0.13H), 7.97–7.28 (m, 8.98H), 7.25–6.95 (m, 11.67H), 6.90 (d, J = 7.5 Hz, 4H), 3.95 (t, J = 12.8 Hz, 6.4 Hz, 3.74H), 1.85–1.71 (m, 3.74H), 1.50–1.27 (m, 18.7H), 0.91–0.84 (t, 5.61H).

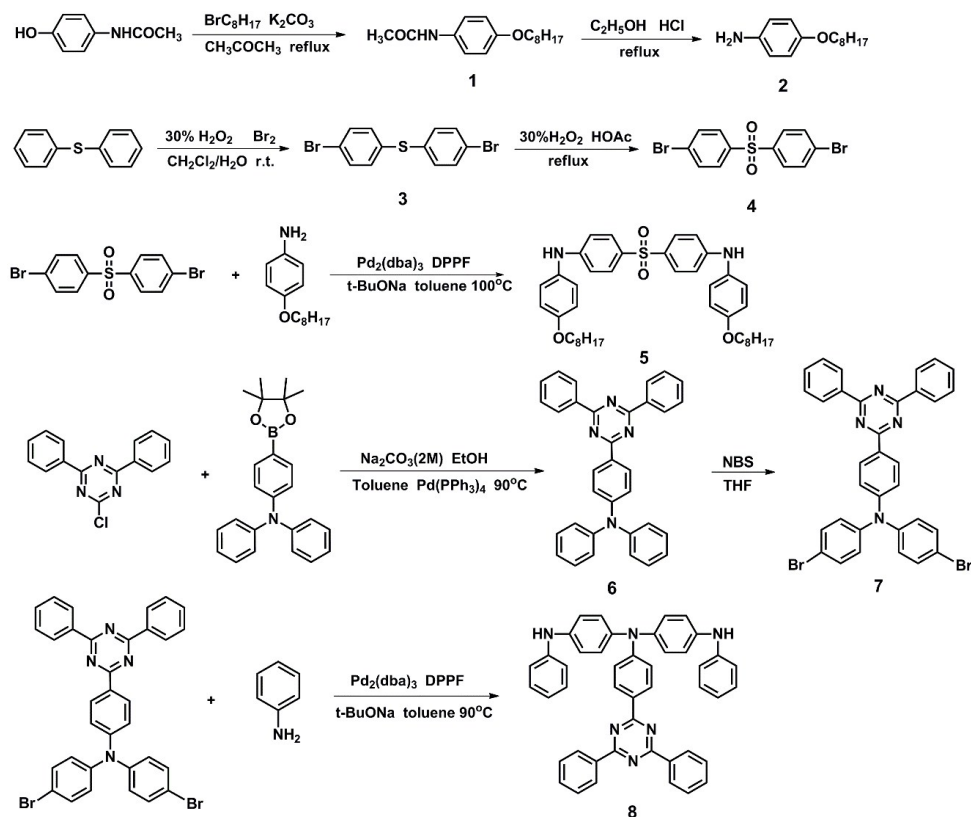
P0: pale yellow powder (yield = 378 mg, 86.6%). **4** (0.1881 g, 0.5 mmol), **5** (0.3285 g, 0.5 mmol) were used in the polymerization. ¹H NMR (500 MHz, CDCl₃): δ 7.83–7.66 (d, 4H), 7.13–7.03 (d, 4H), 7.04–6.98 (d, 2H), 6.92–6.85 (d, 2H), 3.95 (t, J = 6.5 Hz, 2H), 1.82–1.74 (m, 2H), 1.47–1.27 (m, 10H), 0.88 (t, J = 6.6 Hz, 3H).

P2: yellow powder (yield = 372 mg, 85.2%). **4** (0.1881 g, 0.5 mmol), **5** (0.2956 g, 0.45 mmol) and **8** (0.0329 g, 0.05 mmol) were used in the polymerization. ¹H NMR (500 MHz, CDCl₃): δ 8.74 (d, J = 6.9 Hz, 0.46H), 8.65 (d, J = 8.6 Hz, 0.23H), 7.93–7.34 (m, 9.33H), 7.21–6.98 (m, 11.89H), 6.91 (d, J = 21.9 Hz, 15.6 Hz, 4H), 3.95 (t, J = 12.9 Hz, 6.4 Hz, 3.54H), 1.81–1.75 (m, 3.55H), 1.49–1.27 (m, 17.71H), 0.88 (t, J = 6.5 Hz, 5.31H).

P3: yellow powder (yield = 364 mg, 83.5%). **4** (0.1881 g, 0.5 mmol), **5** (0.2792 g, 0.425 mmol) and **8** (0.0494 g, 0.075 mmol) were used in the polymerization. ¹H NMR (500 MHz, CDCl₃): δ 8.74 (d, J = 6.7 Hz, 0.64H), 8.66–8.62 (d, 0.32H), 7.93–7.31 (m, 9.45H), 7.22–6.99 (m, 12.16H), 6.97–6.80 (d, 4H), 3.95 (t, J = 12.9 Hz, 6.4 Hz, 3.36H), 1.81–1.74 (m, 3.35H), 1.47–1.27 (m, 16.81H), 0.88 (t, J = 6.5 Hz, 5.05H).

P4: yellow powder (yield = 386 mg, 88.6%). **4** (0.1881 g, 0.5 mmol), **5** (0.2628 g, 0.4 mmol) and **8** (0.0659 g, 0.1 mmol) were used in the polymerization. ¹H NMR (500 MHz, CDCl₃): δ 8.74 (d, J = 5.4 Hz, 0.85H), 8.66–8.61 (d, 0.43H), 7.93–7.33 (m, 9.78H), 7.21–6.99 (m, 12.32H), 6.95–6.77 (d, 4H), 4.00–3.87 (t, 3.15H), 1.78 (m, J = 3.9 Hz, 3.13H), 1.47–1.26 (m, 15.72H), 0.89 (t, J = 6.0 Hz, 4.73H).

Synthetic route



2. Determination of Φ_{RISC} , Φ_{ISC} , ΔE_{ST} , Rate Constants

As reported previously, the individual PLQYs of fluorescence (Φ_p) and TADF (Φ_d) can be distinguished from the total PLQY (Φ) by comparing the integrated intensities of the prompt and delayed components in the transient photoluminescence spectra (Table S1). Assuming that the nonradiative decay from S1 to S0 is negligible, we can estimate the efficiency of RISC (Φ_{RISC}) and ISC (Φ_{ISC}) using the following equations^{1,2}:

$$\Phi_{\text{ISC}} = 1 - \Phi_p \quad \text{Eq. (1)}$$

$$\Phi_{\text{RISC}} = \Phi_d / (1 - \Phi_p) \quad \text{Eq. (2)}$$

The Φ_{ISC} and Φ_{RISC} values of P0, P1, P2, P3, and P4 doped into mCP films were calculated to be 90% and 16%, 87% and 59%, 90% and 68%, 91% and 79%, and 92% and 72%, respectively (Table S1), which indicates that 10% of the singlet excitons directly underwent radiative decay and 90% of the singlet excitons gave the T1 state through ISC; meanwhile, 16% of the triplet excitons were upconverted into the S1 state and decayed radiatively, e.g., for P0. In addition, because solvent glasses can restrict the rotational relaxation of P0–P4 in the excited state, the ΔE_{ST} of these polymers in doped films at room temperature can be reliably estimated using an approximate relationship between ΔE_{ST} , k_d , and k_p as follows³:

$$k_p = \Phi_p / \tau_p \quad \text{Eq. (3)}$$

$$k_d = \Phi_d / \tau_d \quad \text{Eq. (4)}$$

$$k_d = (1/3)[k_p \exp(-\Delta E_{\text{ST}}/RT)] \quad \text{Eq. (5)}$$

where R and T represent the ideal gas constant and absolute temperature, respectively. The ΔE_{ST} values of P0, P1, P2, P3, and P4 were calculated to be 0.23, 0.21, 0.19, 0.18, and 0.18 eV (Table S1). With the increasing ratio of the DPA-TRZ emitting unit, ΔE_{ST} gradually became smaller, tending to be stable until P3, which indicated that the adjustment of ΔE_{ST} can be effectively realized by an appropriate charge-transfer strategy. The higher Φ_{RISC} of P1–P4 was attributable to a smaller ΔE_{ST} , and thereby led to a more facile upconversion of T1→S1. To further understand the upconversion phenomenon of P0–P4, the rate constants of ISC (k_{ISC}) and RISC (k_{RISC}) can be estimated based on the following equations²:

$$k_{\text{ISC}} = (\Phi_d k_p) / (\Phi_p + \Phi_d) \quad \text{Eq. (6)}$$

$$k_{\text{RISC}} = (\Phi_{\text{d}} k_{\text{p}} k_{\text{d}}) / (\Phi_{\text{p}} k_{\text{ISC}}) \dots\dots\dots \text{Eq. (7)}$$

The k_{ISC} and k_{RISC} values of P0–P4 were estimated and these are summarized in Table S1. These results further verify that by an appropriate charge-transfer strategy, a higher k_{RISC} can be achieved; furthermore, the RISC process is more efficient with the increasing concentration of the DPA-TRZ emitting unit.

References

- 1 A. Endo, K. Sato, K. Yoshimura, T. Kai, A. Kawada, H. Miyazaki and C. Adachi, *Appl. Phys. Lett.*, 2011, **98**, 083302.
- 2 Y. Tao, K. Yuan, T. Chen, P. Xu, H. Li, R. Chen, C. Zheng, L. Zhang and W. Huang, *Adv. Mater.*, 2014, **26**, 7931-7958.
- 3 Q. Zhang, H. Kuwabara, W. J. P. Jr, S. Huang, Y. Hatae, T. Shibata and C. Adachi, *J. Am. Chem. Soc.*, 2014, **136**, 18070.

Table S1 Rate constants, quantum efficiencies and ΔE_{ST} of P0-P4 in mCP films (10 wt%).

Polymers	Φ (%)	Φ_{p} (%)	Φ_{d} (%)	Φ_{d}/Φ (%)	Φ_{ISC} (%)	Φ_{RISC} (%)	k_{ISC} ($\times 10^7 \text{ s}^{-1}$)	k_{RISC} ($\times 10^4 \text{ s}^{-1}$)	ΔE_{ST} (eV)
P0	24	10	14	58.3	90	16	2.33	0.48	0.23
P1	64	13	51	79.7	87	59	2.53	1.64	0.21
P2	71	10	61	85.9	90	68	2.15	3.21	0.19
P3	81	9	72	88.8	91	79	1.81	5.21	0.18
P4	74	8	66	89.2	92	72	1.78	5.43	0.18

Photophysical Properties

Table S2 Properties of the polymers.

Polymers	$M_{\text{n}}^{[\text{a}]}$ (kg/mol)	$M_{\text{w}}^{[\text{b}]}$ (kg/mol)	PDI ^[c]	$T_{\text{d}}^{[\text{d}]}$ (°C)	triazine unit(mol%) in	
					feed ratio	polymer
P0	11.2	16.6	1.49	364	0	0
P1	12.9	19.0	1.47	401	5	6.5
P2	13.1	19.8	1.51	405	10	11.5
P3	12.5	18.6	1.48	420	15	15.9
P4	10.1	14.0	1.39	426	20	21.2

[a] Number-average molecular weight, [b] Weight-average molecular weight, [c] Polydispersity index, [d] Decomposition temperature (5% weight loss).

Table S3 Photophysical properties of polymers in toluene and neat or doped films at 300K.

Polymers	$\lambda_{\text{ab}}(\text{nm})$ sol/film ^[a]	$\lambda_{\text{em}}(\text{nm})$ sol/film ^[a]	$\Phi^{[\text{a}]}$ (%)	$\Phi_{\text{p}}/\tau_{\text{p}}^{[\text{b}]}$ (%/ns)	$\Phi_{\text{d}}/\tau_{\text{d}}^{[\text{b}]}$ (%/μs)	HOMO ^[c] (eV)	LUMO ^[d] (eV)	$\Delta E_{\text{ST}}^{[\text{e}]}$ (eV)
P0	318 364 /309 365	437 /453(438)	12(24)	10/2.5	14/70.5	5.55	2.57	0.2
P1	318 364 413 /309 365 419	437 515 /516(487)	37(64)	13/4.1	51/152.6	5.55	3.05	0.19
P2	318 364 413 /309 365 419	437 526 /520(493)	36(71)	10/4.0	61/134.9	5.54	3.04	0.18
P3	318 364 413 /309 365 419	437 530 /528(508)	39(81)	9/4.4	72/124.5	5.52	3.02	0.18
P4	318 364 413 /309 365 419	437 531 /529(509)	36(74)	8/4.0	66/112.6	5.49	2.99	0.18

[a] Measured in neat films. The values in parentheses are obtained from 10 wt% doped films in mCP. [b] The fractional contributions of the fluorescence (Φ_p) and TADF (Φ_d) to the total absolute PL quantum yield (Φ) and lifetimes of the prompt (τ_p) and delayed (τ_d) decay components for the 10 wt% doped films measured at 300 K. [c] Determined by cyclic voltammogram in thin films. [d] Deduced from the HOMO and the optical energy gap (E_g) values, which were determined from the onset of the thin film absorption spectra. [e] Evaluated in toluene at 77 K.

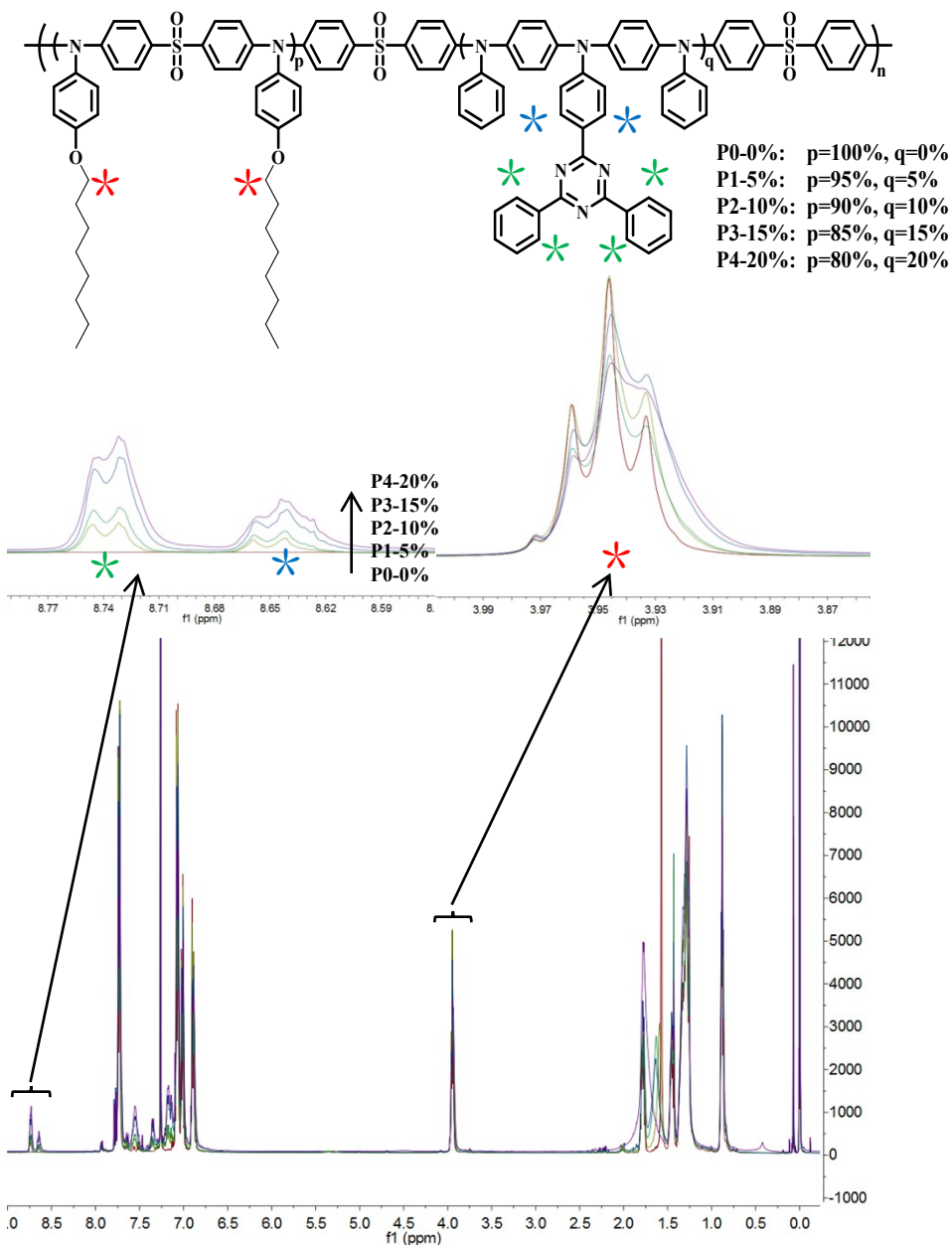


Fig. S1 ^1H NMR spectra of P0-P4. With the increase of the DPA-TRZ emitting unit ratio, the intensities of hydrogen signal at 8.59-8.68 ppm and 8.71-8.77 ppm are gradually increasing.

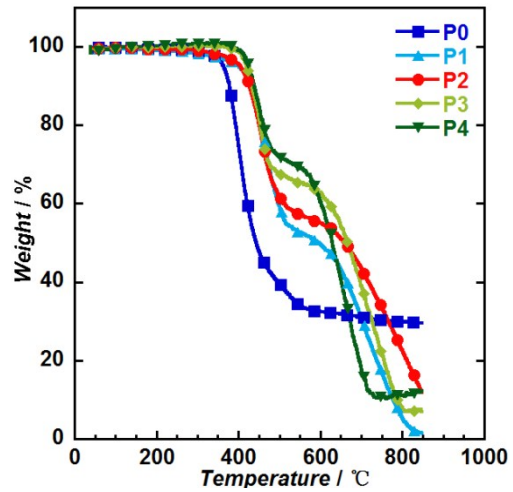


Fig. S2 TGA curves of polymers at a heating rate of 10 °C min⁻¹ under N₂.

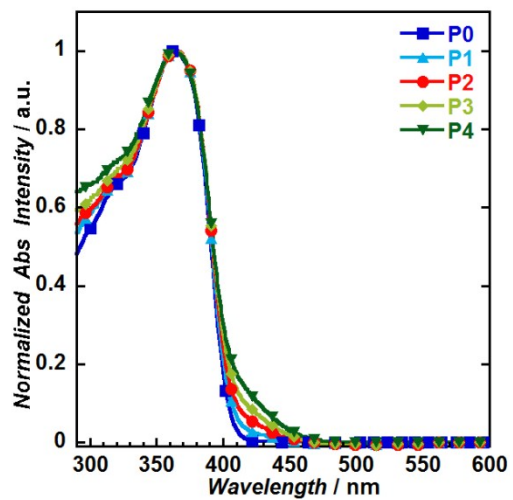


Fig. S3 The UV-vis absorption spectra for P0-P4 in toluene.

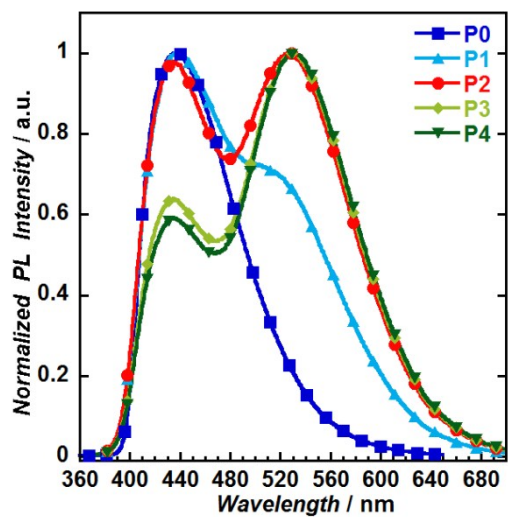


Fig. S4 PL spectra for P0–P4 in toluene.

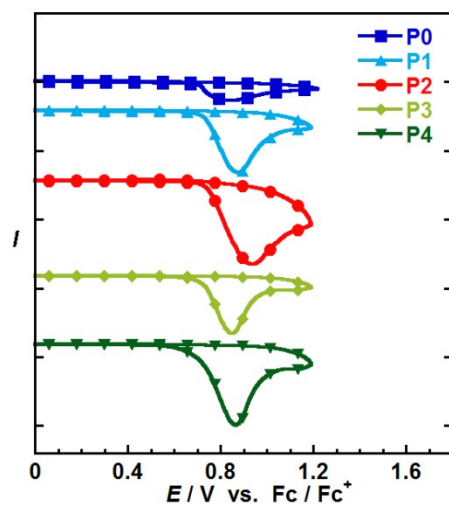


Fig. S5 Cyclic Voltammogram of polymers (oxidation potential).

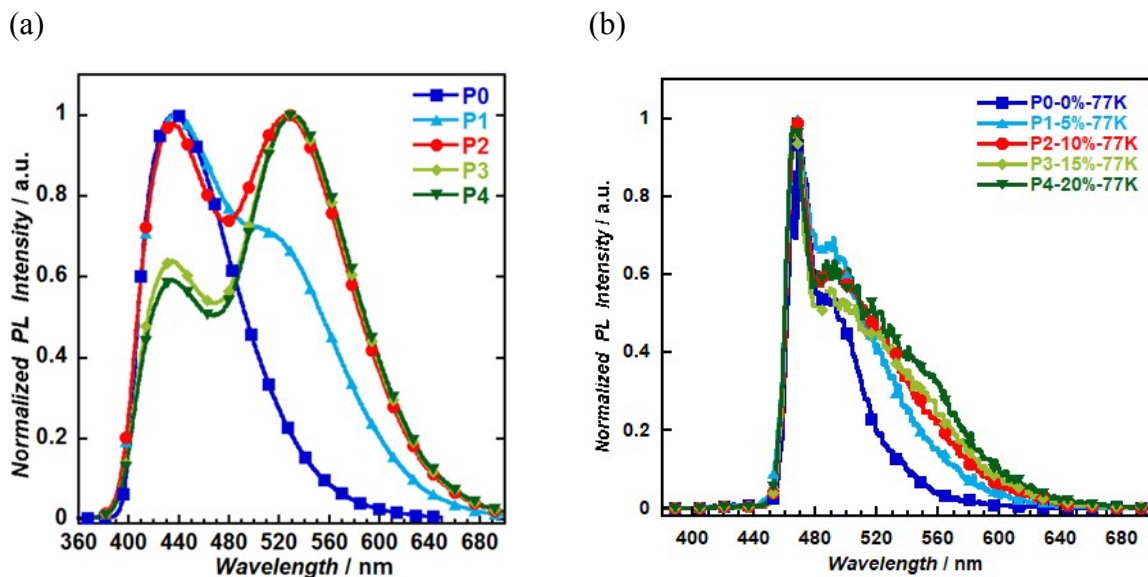


Fig. S6 PL spectra of prompt fluorescence at 300 K (a) and phosphorescence (delayed by 1 ms) at 77 K for polymers in toluene (b). The lowest excited singlet (S1) and triplet energy (T1) levels were determined from the highest energy vibronic band for the fluorescence and phosphorescence, respectively.

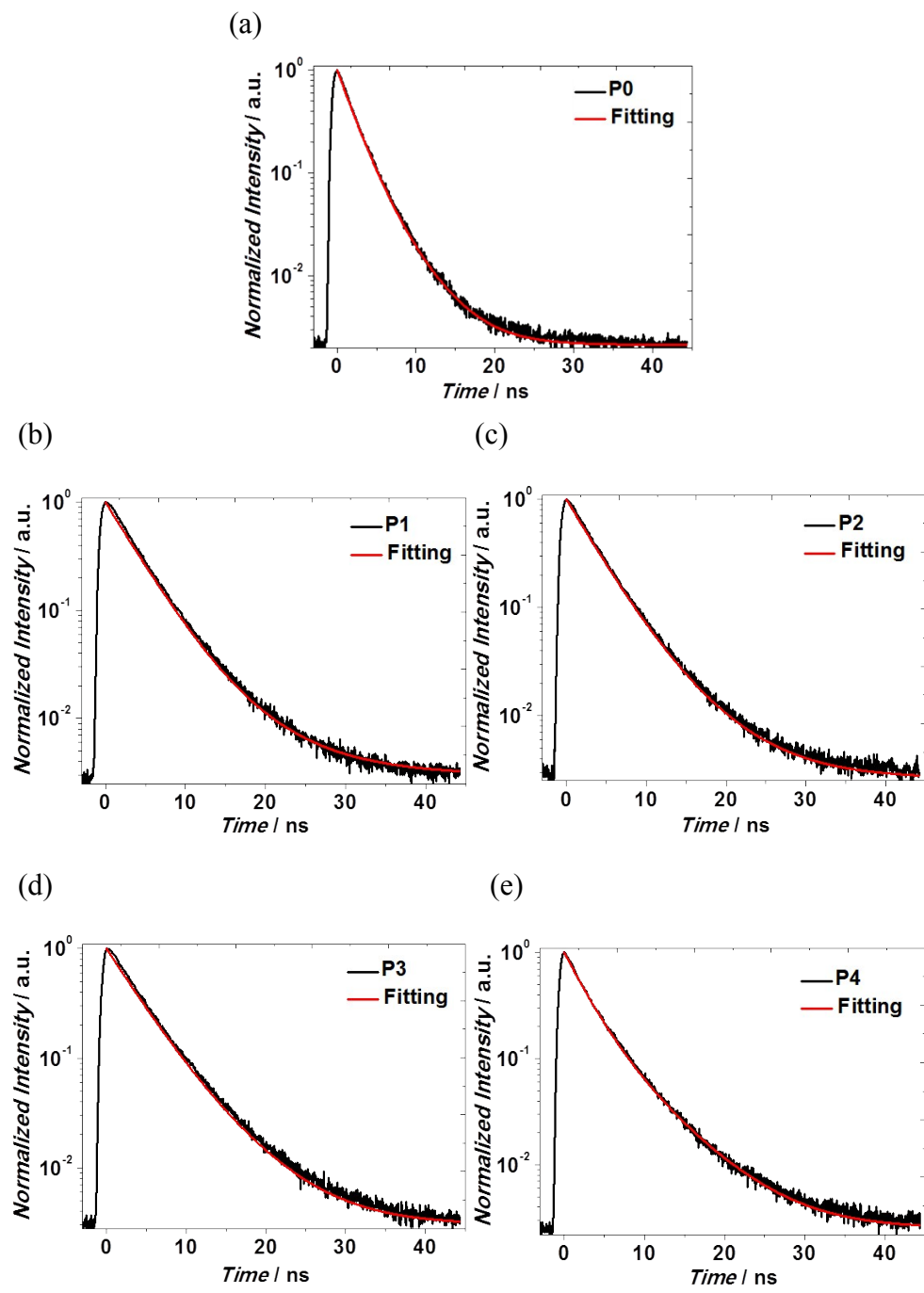


Fig. S7 Prompt emission decay curves of P0–P4 in doped films at 300K.

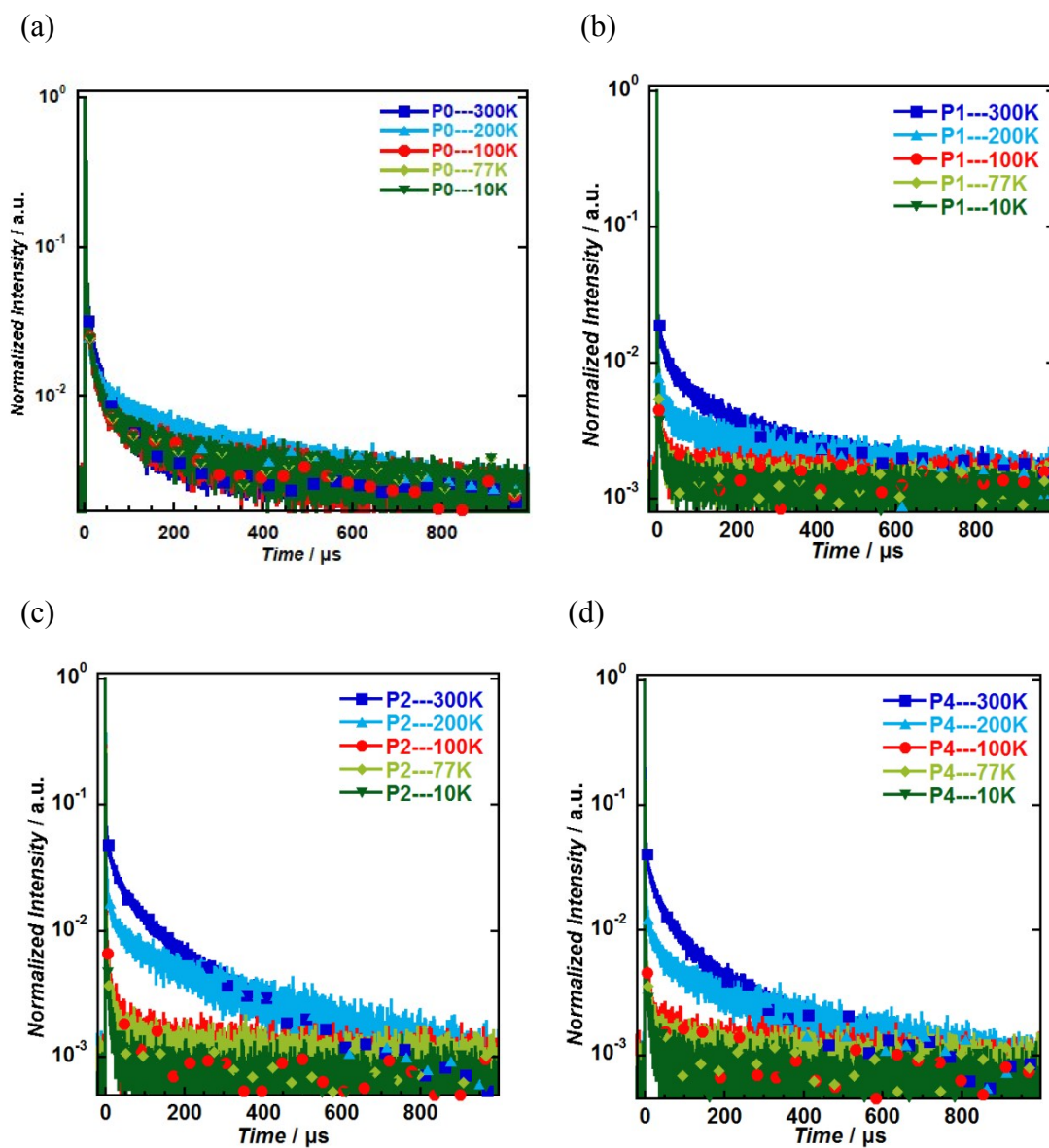


Fig. S8 Temperature dependences of transient PL decays ranging from 10 to 300 K for polymers : mCP doped films.

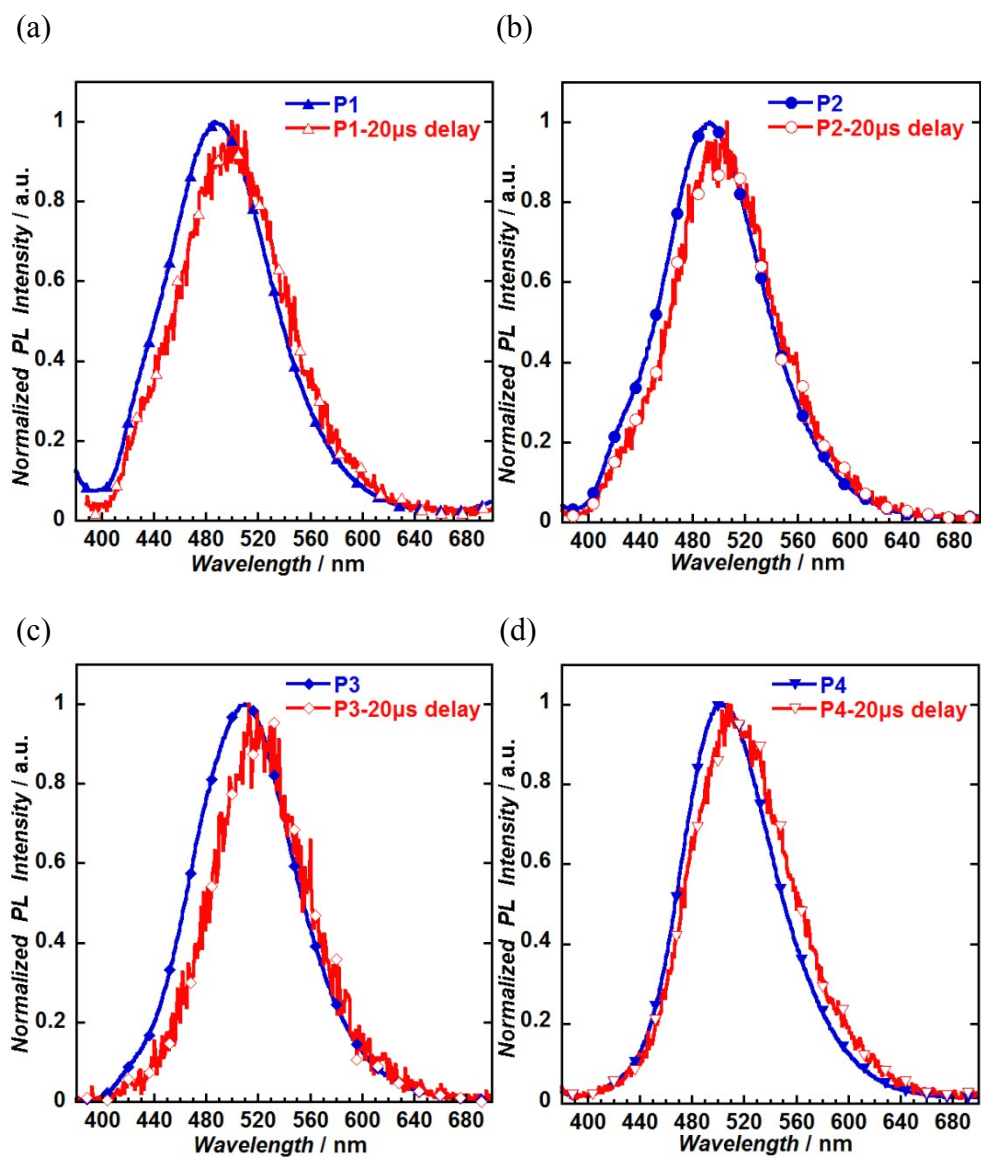


Fig. S9 The photoluminescence spectrum of doped films without delay time and 20 μs delay time at room temperature.

3. Device Fabrication and Performance

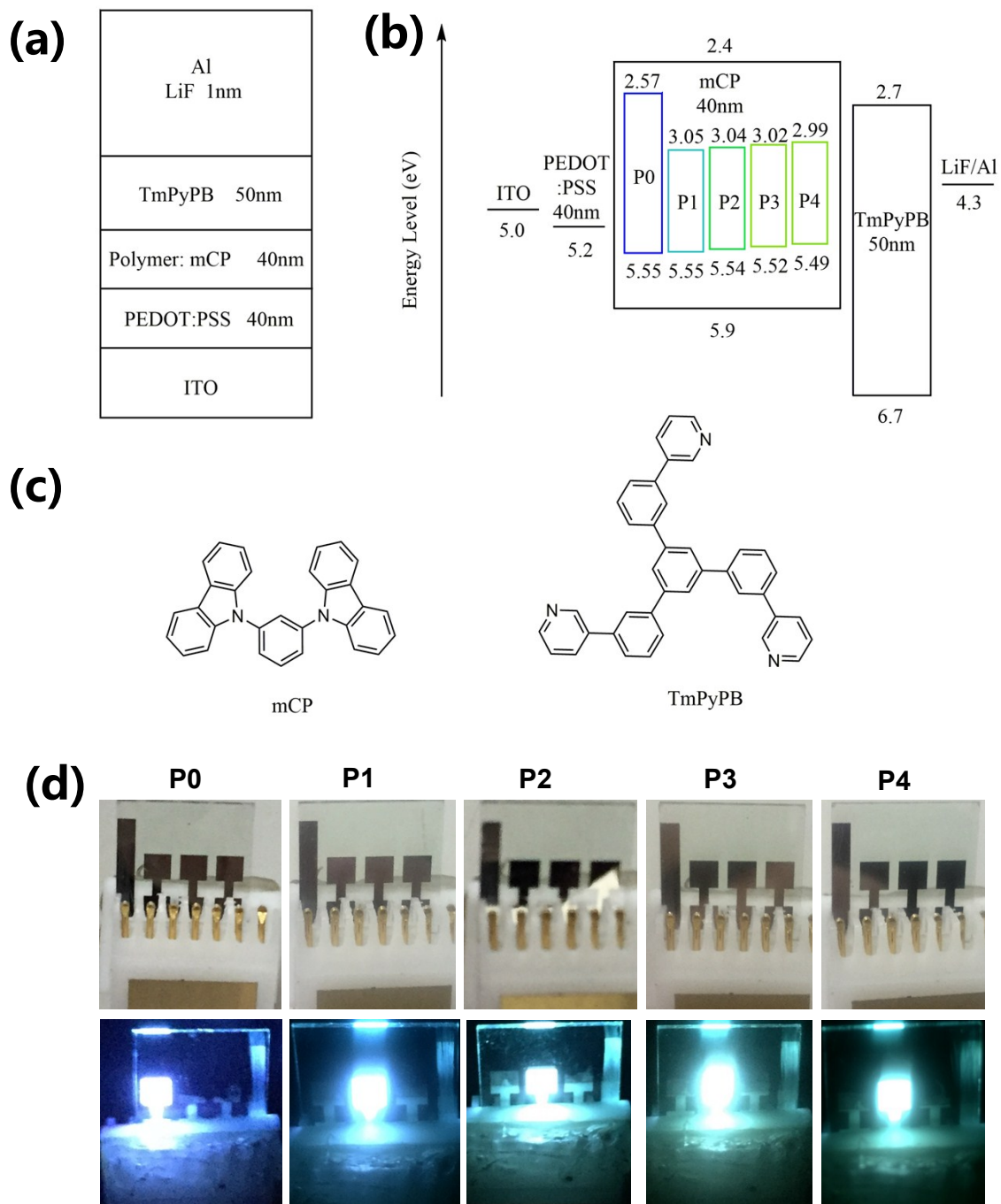


Fig. S10 Device structure of devices (a), energy level alignment of devices (b), the molecular structure of mCP and TmPyPB (c), and the emitting images of the resulting light-emitting devices (d).

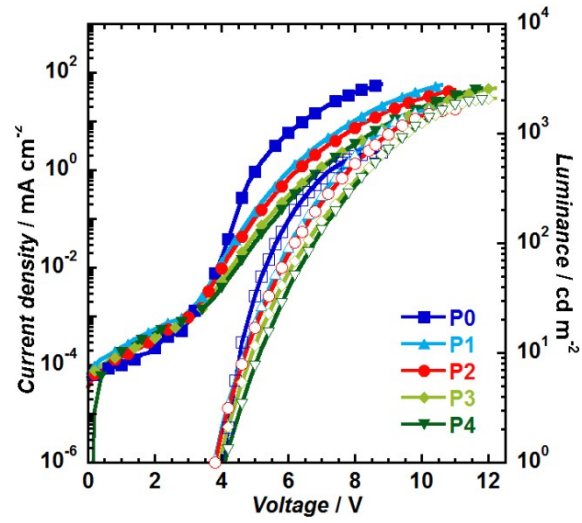


Fig. S11 Current density–voltage–luminance (J–V–L) curves.

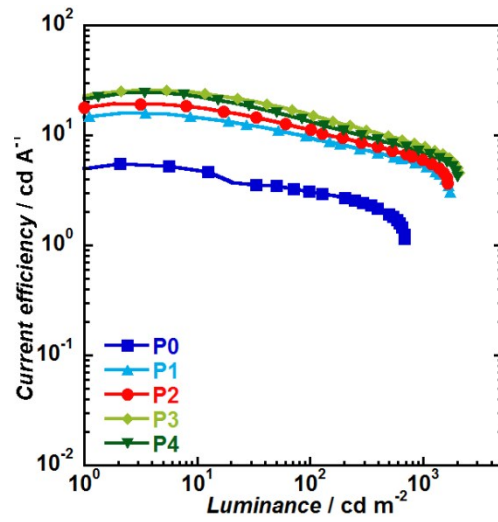


Fig. S12 Current efficiency–luminance characteristics of Devices A ~ E.

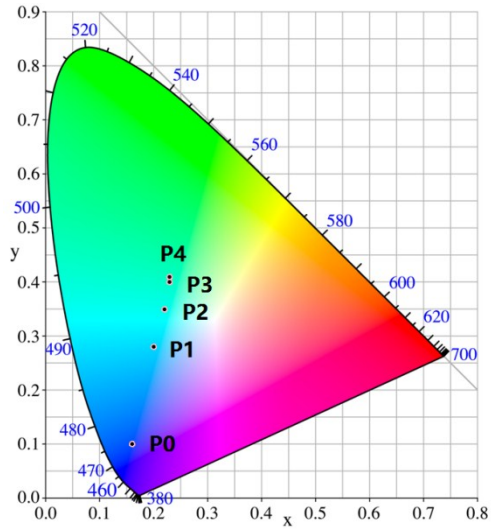
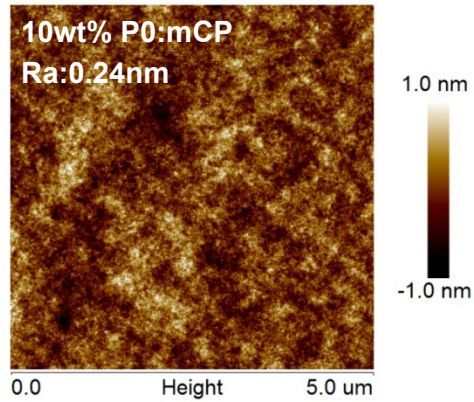


Fig. S13 EL color coordinates on the CIE 1931 chromaticity diagram.

Table S4 Device performance of Devices A ~ E with P0 ~ P4 as the emitters at 100 cd m⁻² and 1000 cd m⁻².

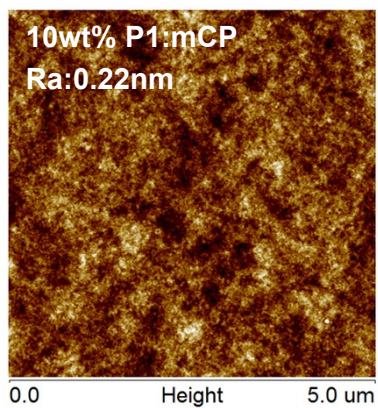
Device	Emitter	at 100 cd m ⁻²				at 1000 cd m ⁻²			
		V (V)	CE (cd/A)	PE (lm/W)	EQE (%)	V (V)	CE (cd/A)	PE (lm/W)	EQE (%)
A	P0	5.6	3.1	1.7	3.0				
B	P1	6.1	9.8	5.0	3.6	8.7	5.4	1.9	2.0
C	P2	6.2	11.2	5.7	4.0	9.0	6.0	2.1	2.1
D	P3	6.6	15.2	7.2	5.1	9.5	8.1	2.7	2.6
E	P4	6.8	13.3	6.1	4.5	9.6	7.0	2.3	2.3

(a)

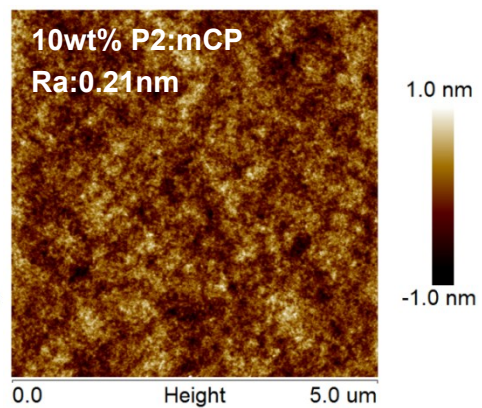


(b)

(c)



(d)



(e)

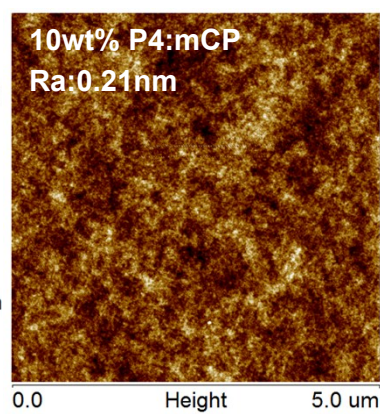
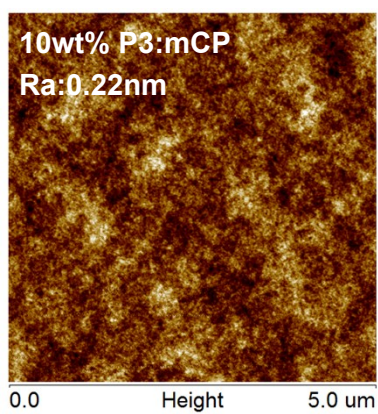


Fig. S14 AFM height images of spin-coated 10wt% polymers : mCP doped films.

4. NMR and MS Spectra

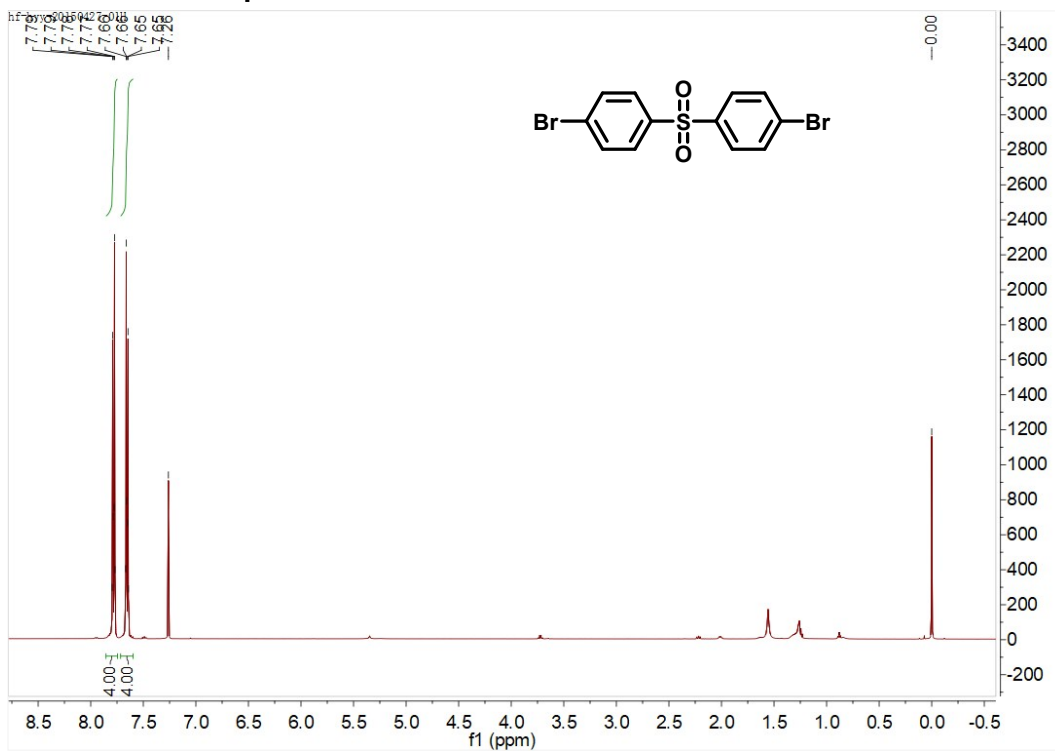


Fig. S15 ^1H NMR spectrum of **4** in CDCl_3 .

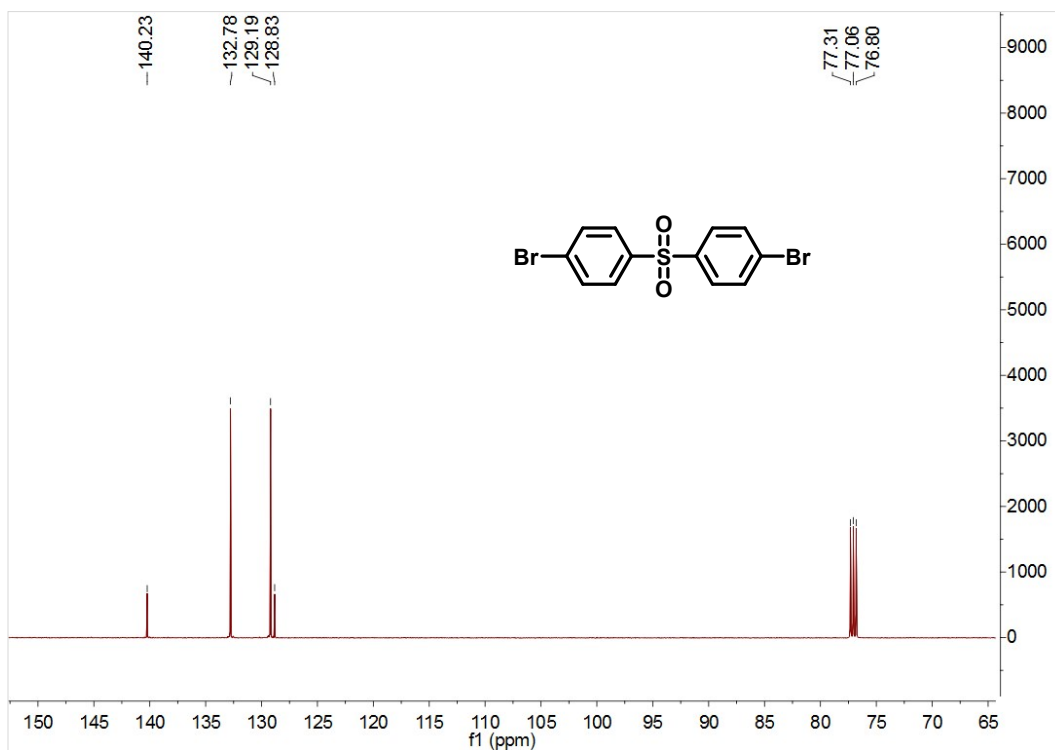


Fig. S16 ^{13}C NMR spectrum of **4** in CDCl_3 .

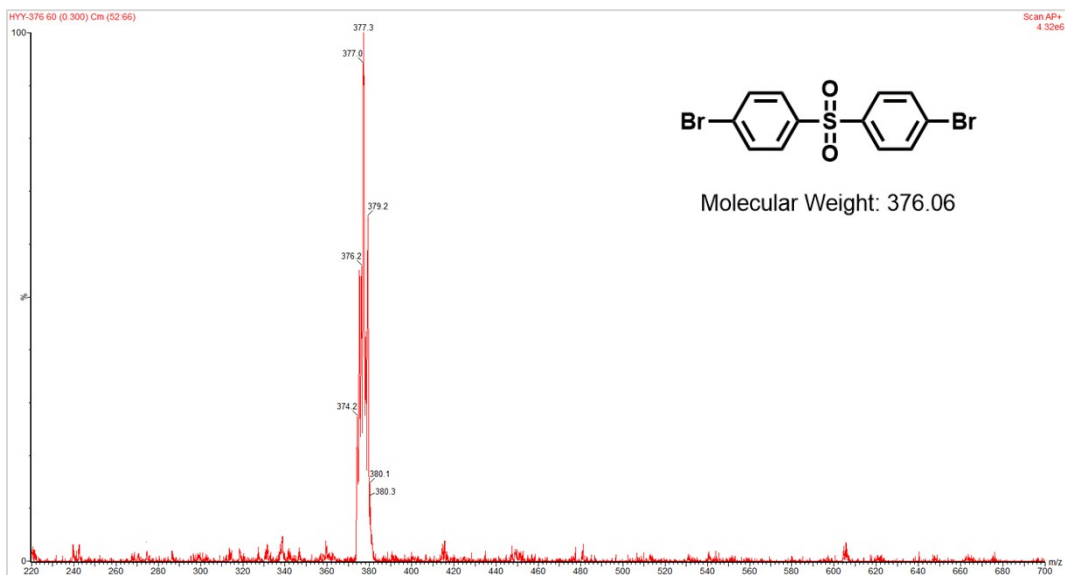


Fig. S17 LC-MS of 4.

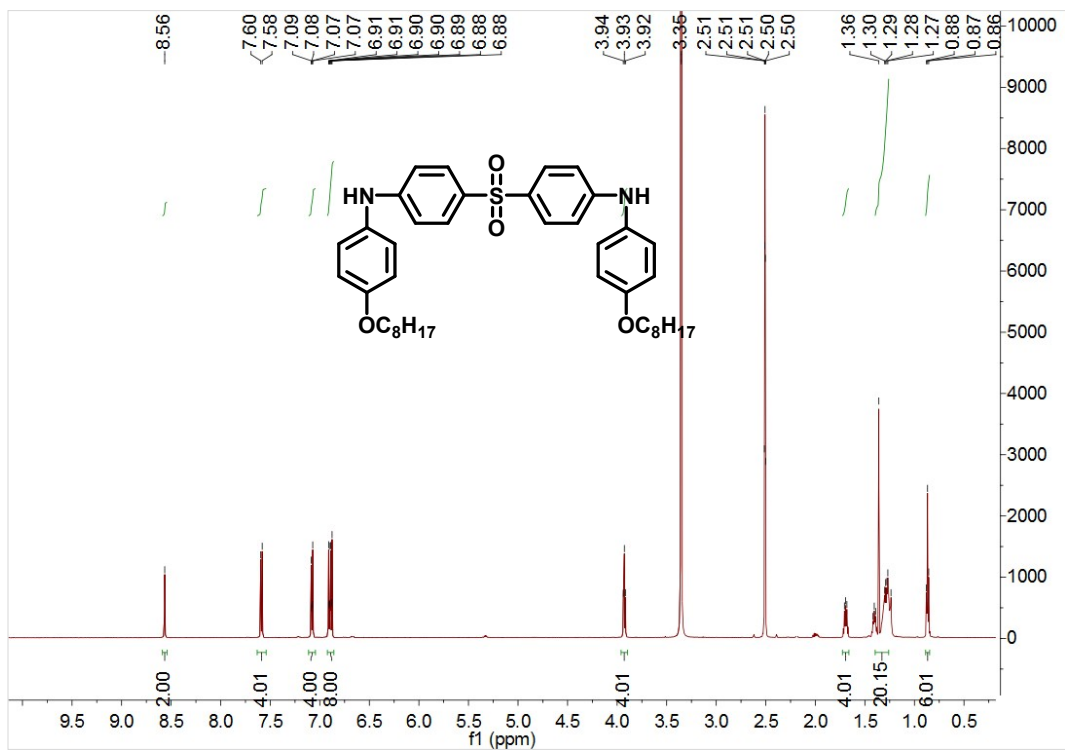


Fig. S18 ¹H NMR spectrum of 5 in DMSO-*d*₆.

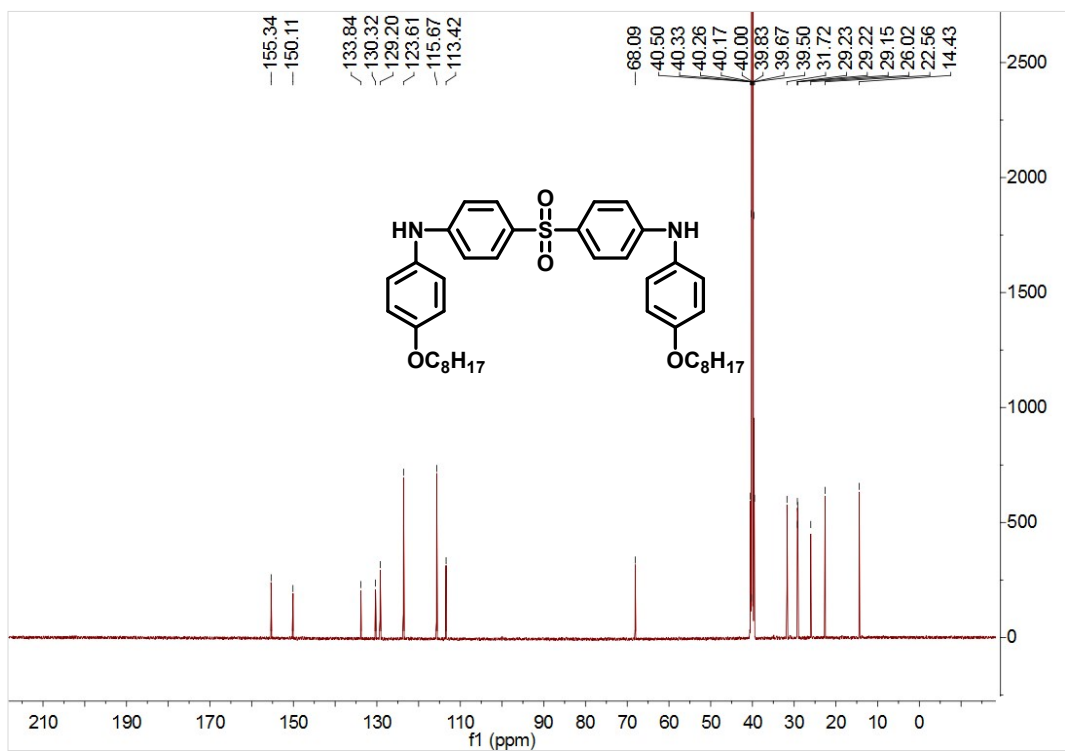


Fig. S19 ¹³C NMR spectrum of **5** in DMSO-*d*₆.

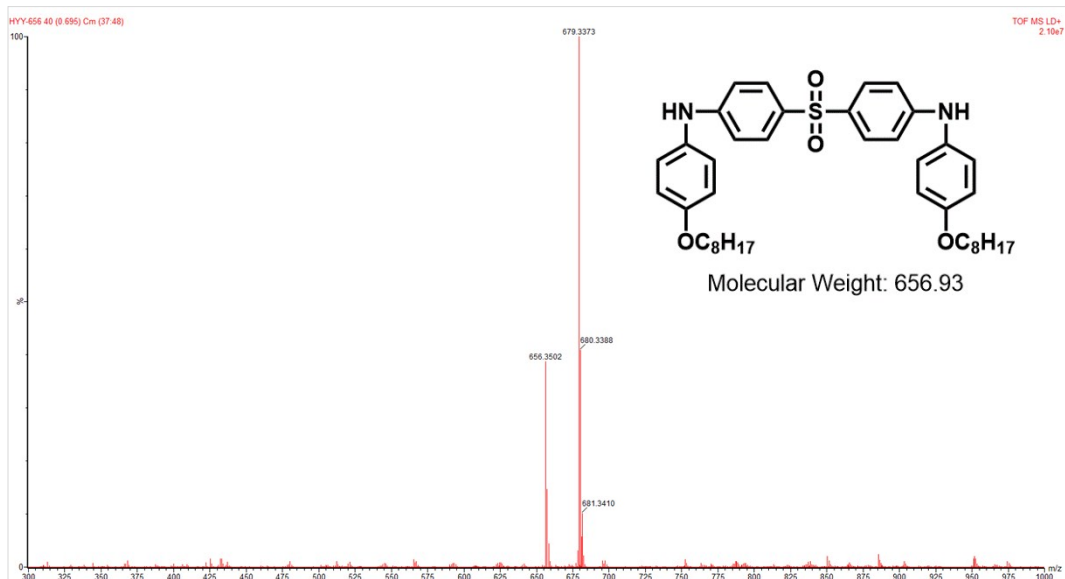


Fig. S20 MALDI-TOF-MS of **5**.

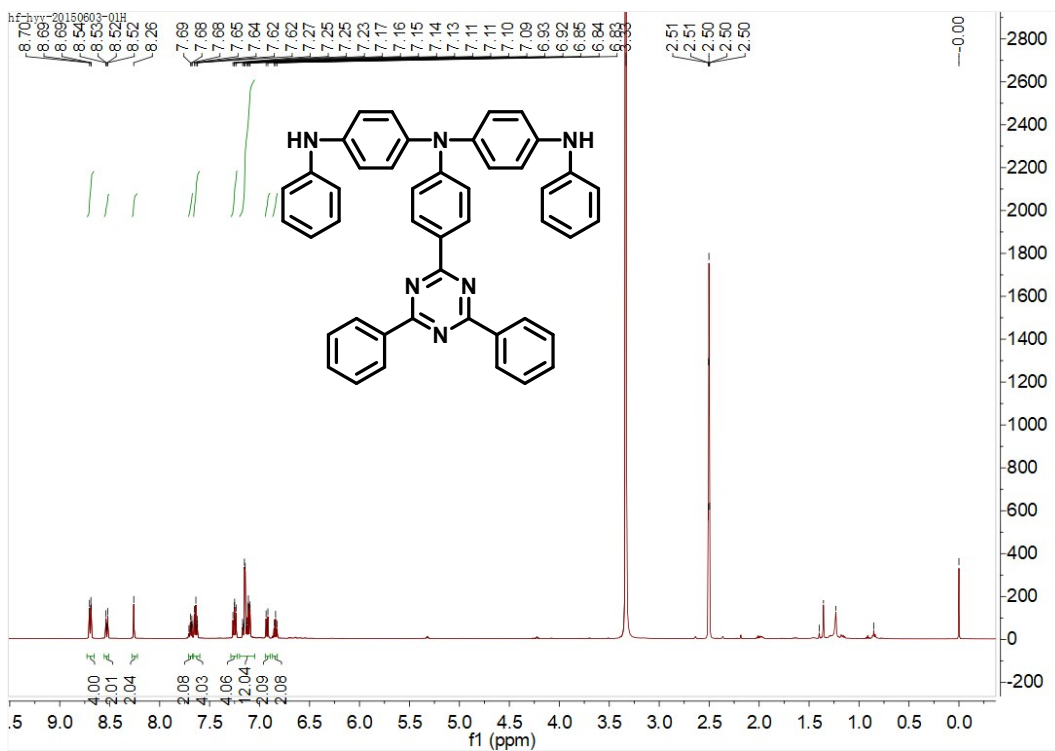


Fig. S21 ^1H NMR spectrum of **8** in $\text{DMSO-}d_6$.

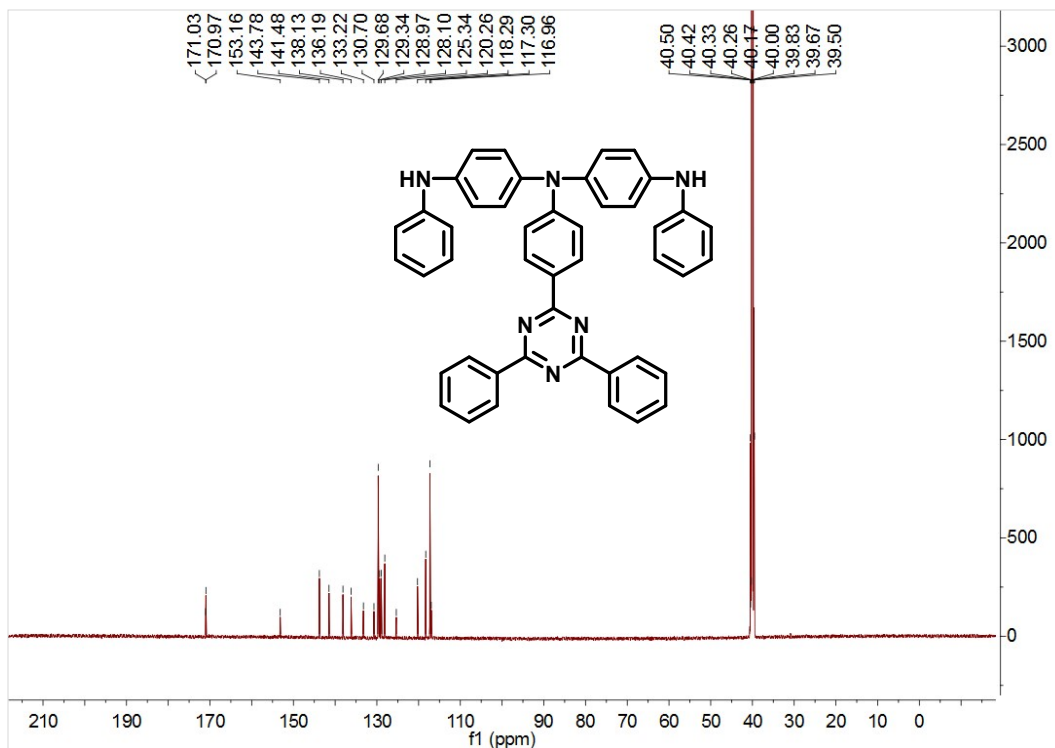


Fig. S22 ^{13}C NMR spectrum of **8** in $\text{DMSO-}d_6$.

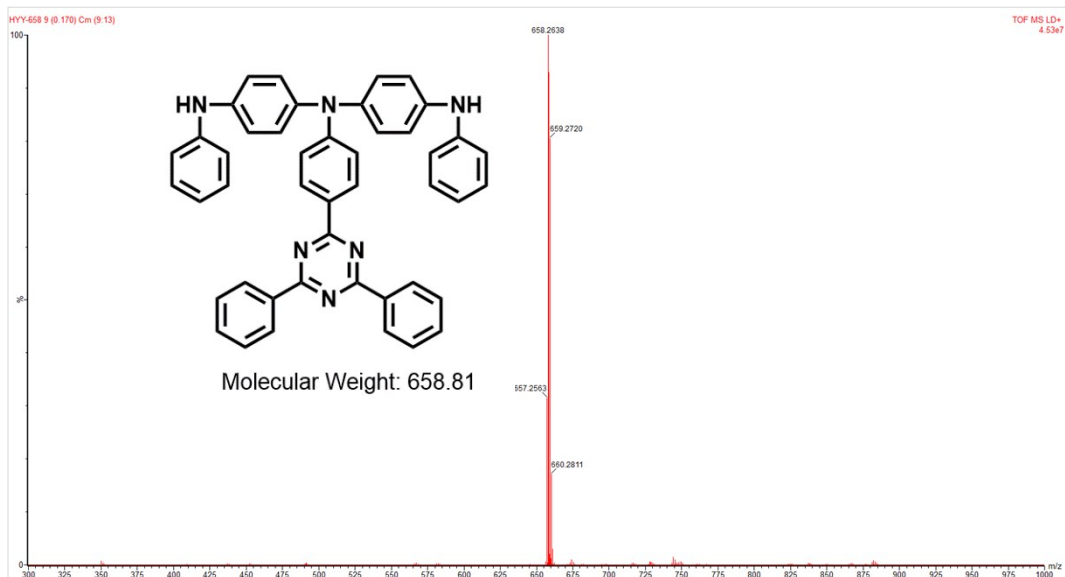


Fig. S23 MALDI-TOF-MS of **8**.

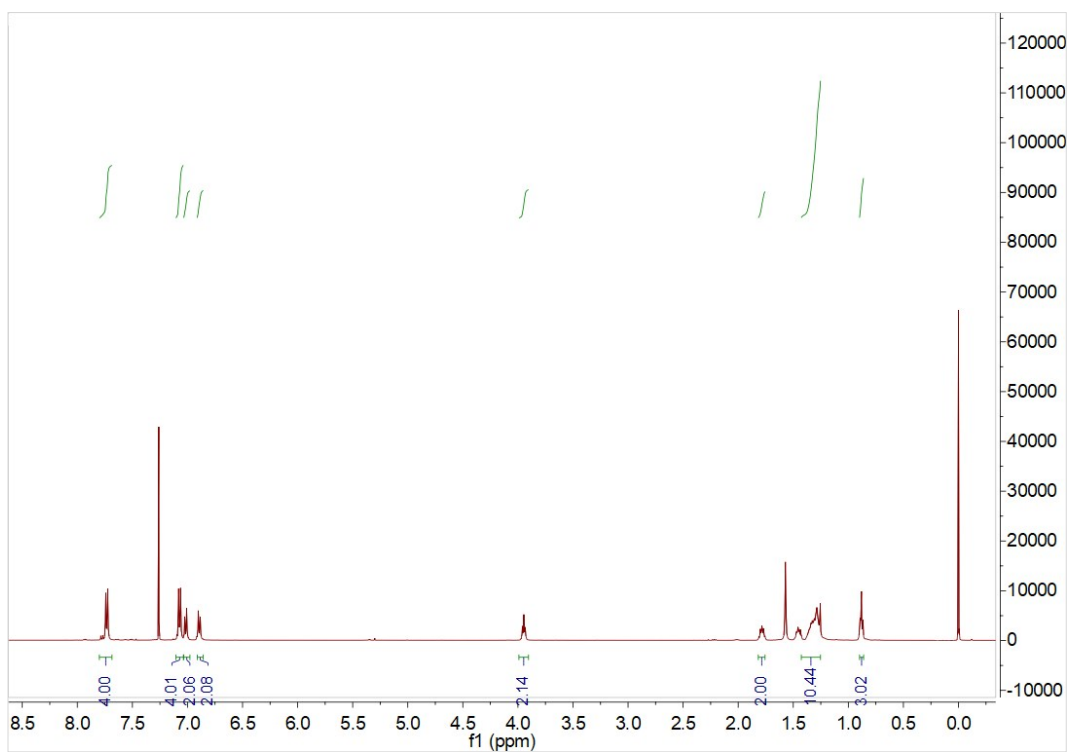


Fig. S24 ¹H NMR spectrum of **P0** in CDCl₃.

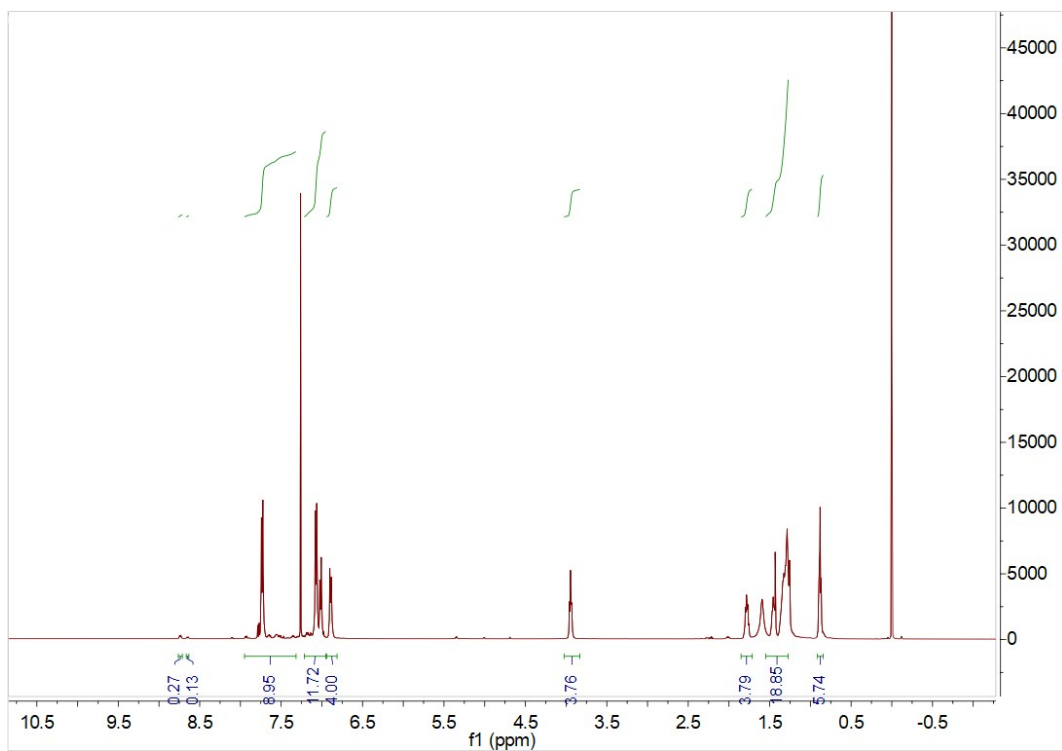


Fig. S25 ¹H NMR spectrum of P1 in CDCl₃.

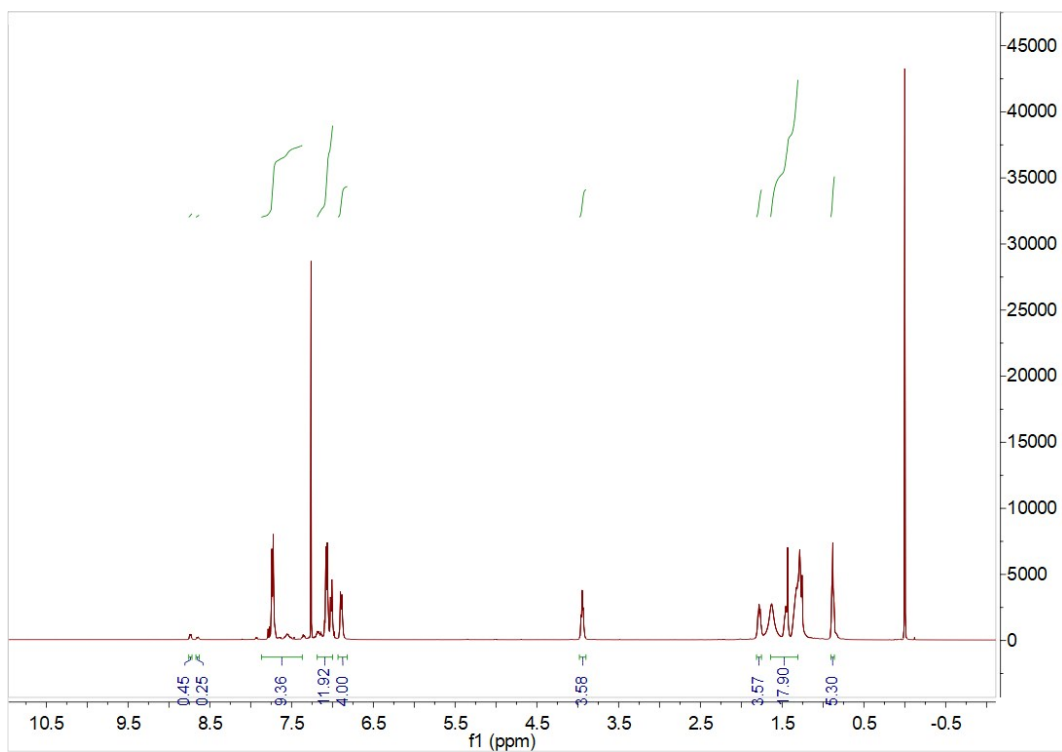


Fig. S26 ¹H NMR spectrum of P2 in CDCl₃.

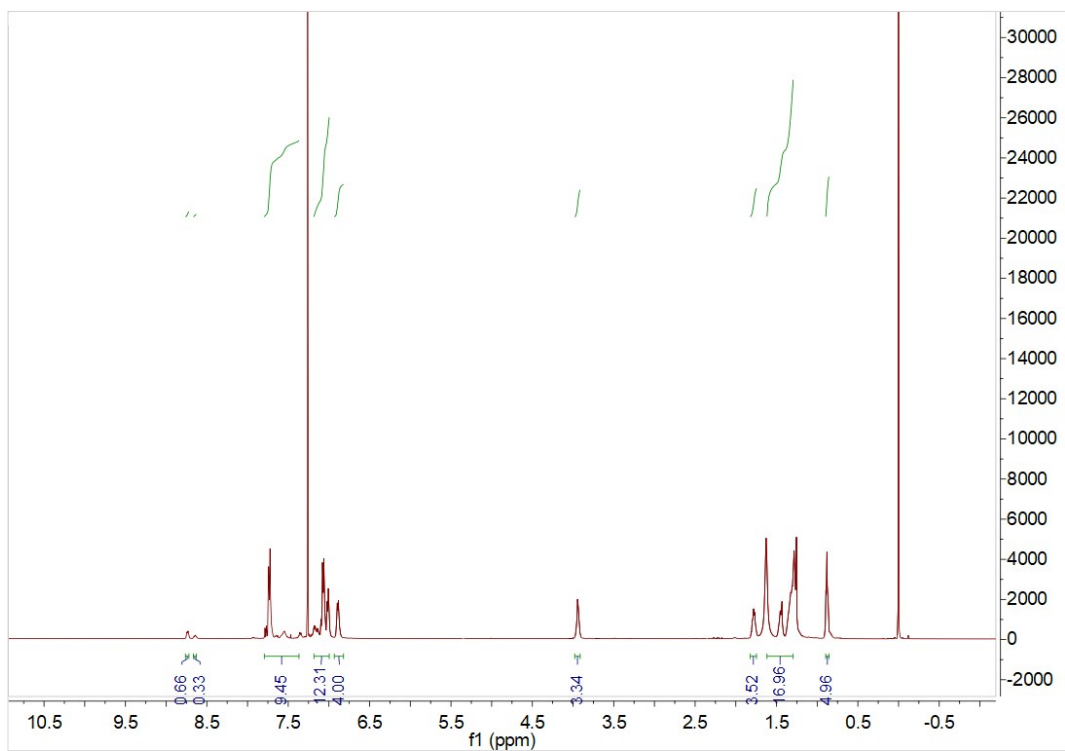


Fig. S27 ^1H NMR spectrum of **P3** in CDCl_3 .

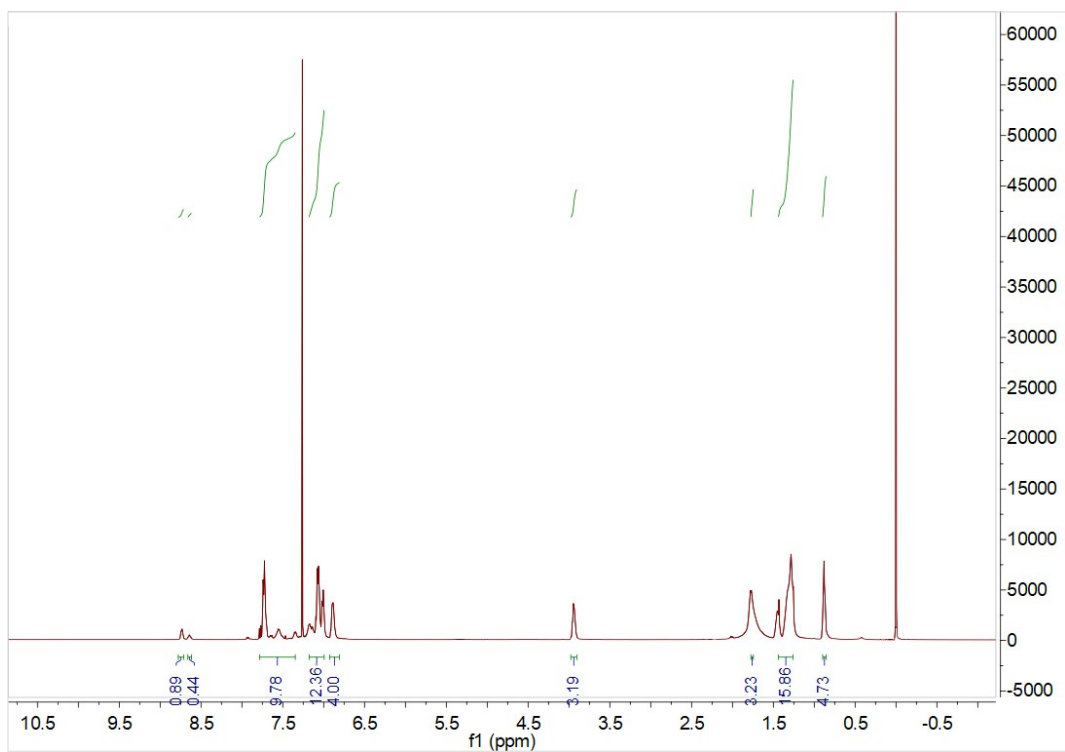


Fig. S28 ^1H NMR spectrum of **P4** in CDCl_3 .